International Journal of Control, Automation and Systems 19(5) (2021) 1863-1872
http://dx.doi.org/10.1007/s12555-019-0535-1

ISSN:1598-6446 eISSN:2005-4092
http://www.springer.com/12555

Estimation of the Shapley Value of a Peer-to-peer Energy Sharing Game Using Multi-Step Coalitional Stratified Sampling

Liyang Han*, **Thomas Morstyn, and Malcolm McCulloch**

Abstract: One of the main objectives of a peer-to-peer energy market is to efficiently manage distributed energy resources while creating additional financial benefits for the participants. Cooperative game theory offers such a framework, and the Shapley value, a cooperative game payoff allocation based on the participants' marginal contributions made to the local energy coalition, is shown to be fair and efficient. However, its high computational complexity limits the size of the game. In order to improve this peer-to-peer cooperative scheme's scalability, this paper investigates and adapts a stratified sampling method for the Shapley value estimation. It then proposes a multi-step sampling strategy to further reduce the computation time by dividing the samples into incremental parts and terminating the sampling process once a certain level of estimation performance is achieved. Finally, selected case studies demonstrate the effectiveness of the proposed method, which is able to scale up the game from 20 players to 100 players.

Keywords: Cooperative game theory, energy management, energy storage, P2P energy sharing, Shapley value.

1. INTRODUCTION

The increasing penetration of distributed energy resources (DER) poses challenges to distribution network operation. One of the most important topics recent researches have been focusing on is how to maintain the reliability of energy supply while encouraging distributed renewable generation, which is highly variable and intermittent [1]. Curtailment is applied in some networks with high renewable generation [2]. However, it introduces inefficiency into the energy system and financially penalizes owners of renewable resources. Centralized control of DER is also proposed in various researches, but they are limited by their scalability [3]. Distributed control systems are able to coordinate DER efficiently in real-time to maintain the network stability [4], but they tend to overlook the fact that prosumers, proactive-consumers with distributed energy resources that actively control their energy behaviors, are independent entities who need incentives to participate in such a centralized control scheme [5]. The concept of peer-to-peer (P2P) energy markets has gained tremendous attention both in the industry and in academia in recent years, as it is considered a key market strategy to financially encourage efficient distributed management of DER [6].

A key feature of a P2P sharing scheme is its ability to use local flexibility to offset generation uncertainty, [7]. Local flexibility often takes the form of energy storage (ES), which can be modeled in a similar way as other types of flexible demand [8]. With the fast increasing amount of distributed generation, the price to export energy has largely fallen below the price to import [9,10]; hence, for a single prosumer, the benefit of flexibility is easily reflected in their energy bills when they increase the local usage of their own generation by optimally scheduling their ES systems [11]. In a P2P market, where local flexibility and variable generation can be matched among participants, additional joint benefits can be created [12]. At the same time, however, it becomes a challenge to allocate these additional benefits to each participant in an efficient and fair way.

Game theory is adopted in some recent P2P market studies to formulate financial incentives to affect prosumer behavior. Dynamic pricing is often coupled with non-cooperative game theoretic frameworks [13–15]. Using an iterative process to update the prices based on prosumer operation decisions in each iteration, these schemes seek

Manuscript received July 16, 2019; revised May 15, 2020; accepted August 25, 2020. Recommended by Associate Editor Soohee Han under the direction of Editor-in-Chief Keum-Shik Hong. This work was supported in part by the Engineering and Physical Sciences Research Council under Grants EP/N03466X/1, EP/S000887/1, and EP/S031901/1, and in part by the Oxford Martin Programme on Integrating Renewable Energy.

Liyang Han is with the Department of Electrical Engineering, Technical University of Denmark, 2800 Lyngby, Denmark (e-mail: liyha@elektro.dtu.dk). Thomas Morstyn is with the School of Engineering, University of Edinburgh, Edinburgh EH9 3JL, U.K. (e-mail: thomas.morstyn@ed.ac.uk). Malcolm McCulloch is with the Department of Engineering Science, University of Oxford, Oxford OX1 2JD, U.K. (e-mail: malcolm.mcculloch@eng.ox.ac.uk).
* Corresponding author.

to find an equilibrium, where no player can be financially better of deviating from said operation [16]. Even though a non-cooperative game theoretic scheme can be solved in a distributed fashion [17], and is able to achieve the maximum welfare at the system level [18], it does not offer the flexibility at market equilibrium to redistribute the benefits [19], causing concerns about fairness. Cooperative game theory, on the other hand, focuses on allocating the maximized joint benefits among the participants to meet certain social criteria, such as fairness, and is thus adopted to construct P2P markets as well [20–23]. It is shown in [20] that financial rewards can be guaranteed and fairly allocated using the Shapley value, which is computed based on the contribution each prosumer makes to the cooperative scheme.

A player's Shapley value in a cooperative game is the weighted average of their marginal contribution to all the possible coalitions that can be constructed among all players [24]. In other words, for an N-player game, the values of all 2^N possible coalitions need to be computed. This means that the computation of the Shapley value becomes intractable when increasing the number of players. In order to overcome the computational issue, [25] uses a sample-based approximation of the Shapley value of the cooperative scheme, which is constructed as simple games with binary outcomes representing whether a coalition of battery-owning households can overcome a hard network constraint. However, this is not a full P2P market scheme as it overlooks the potential contributions made by local generation and small ES systems. The computational complexity is a limiting factor in all the cooperative game theoretic P2P schemes that incorporate both distributed generation and ES systems [21–23], and the largest number of participants demonstrated in these studies is only 15.

Not limiting to the application of cooperative game theory in P2P markets, techniques to estimate the Shapley value have been explored in some previous literature, sampling being the main methodology. A random sampling method for the Shapley value estimation was proposed in [26], and then modified in [27] by adding a stratification step to improve the accuracy of the estimation.

To improve the scalability of the P2P cooperative game proposed in the authors' previous work [23], this paper formulates a novel coalitional stratified sampling method to estimate the Shapley value. It adapts the existing random sampling methods by creating *coalitional strata* and comparing their sizes with the preset sample size to customize the sample size for each coalitional stratum. Additionally, the paper proposes a novel multi-step sampling strategy to further reduce the computation time. This multi-step sampling strategy provides a metric to measure the estimation accuracy and terminates the sampling process when the desired accuracy is achieved. The proposed method is shown in case studies to outperform existing methods both in terms of the computation time and the estimation accuracy. To the best of the authors' knowledge, this is the first time the sampling method is used in constructing a scalable cooperative P2P market scheme. With a realistically sized P2P market (>50 participants), it is then possible to analyze the impact of different DER adoption rates on prosumer profitability. Some interesting findings are shown in the case studies.

2. P2P COOPERATIVE GAME

In an N-player cooperative game, the *grand coalition* $\mathcal{N}$ is defined as the group of all N players. Any subset of the *grand coalition* $\mathcal{T} : \mathcal{T} \subseteq \mathcal{N}$ is called a *coalition*. The basic framework of the P2P cooperative game proposed in [23] involves mainly three steps. Step 1 is to cooperatively manage DER within all coalitions, which requires optimally scheduling the ES units to minimize the *coalitional energy cost*, see Subsection 2.1. Step 2 is to quantify the value of forming each coalition, see Subsection 2.2. Step 3 is to divide the total energy cost savings from forming the *grand coalition* to all the players based on certain criteria, see Subsection 2.3.

2.1. Coalitional energy management

We index each prosumer by i and the *grand coalition* by $i \in \mathcal{N} := \{1,2,...,N\}$. If we consider K timesteps ($t = 1,2,...,K$) with a time interval of Δt, the total energy cost of a coalition $\mathcal{T}$ can be written as

$$F_{\mathcal{T}}(\mathbf{b}) = \sum_{t=1}^{K}\sum_{i\in\mathcal{T}}\left\{r_t^{im}[p_{it}+b_{it}]^{+} + r_t^{ex}[p_{it}+b_{it}]^{-}\right\},$$

where *subscripts* i and t are indices for the player and the timestep respectively. The known inputs are r_t^{im}, r_t^{ex}, and p_{it}, which are electricity import price (£/kWh), electricity export price (£/kWh), and net energy consumption (positive) or generation (negative) (kWh) without ES. The variables are $\mathbf{b} \in \mathbb{R}^{N\times K} := b_{it}, \forall i \in [1,N], \forall t \in [1,K]$: ES charge (positive) or discharge (negative) energy (kWh). We also define operation $[z]^{+(-)} = \max(\min)\{z,0\}$.

With the assumption $r_t^{im} > r_t^{ex}, \forall t$, we can schedule all the ES units' operation within coalition $\mathcal{T}$ to minimize the *coalitional energy cost* $G(\mathcal{T})$, which is defined as

$$G(\mathcal{T}) = \min_{\mathbf{b}} F_{\mathcal{T}}(\mathbf{b})$$

$$s.t.\quad \underline{b}_i \le b_{it} \le \overline{b}_i,\ \ \forall i \in \mathcal{T}, \forall t \in [1,K], \tag{1}$$

$$e_i\underline{SoC}_i \le e_iSoC_i^0 + \sum_{t=1}^{k}([b_{it}]^{+}\eta_i^{in} + [b_{it}]^{-}/\eta_i^{out}) \le e_i\overline{SoC}_i,\ \ \forall i \in \mathcal{T}, \forall k \in [1,K], \tag{2}$$

$$\sum_{t=1}^{K}([b_{it}]^{+}\eta_i^{in} + [b_{it}]^{-}/\eta_i^{out}) = 0,\ \ \forall i \in \mathcal{T}, \tag{3}$$

where (1), (2), and (3) represent the ES power constraint, energy constraint, and cycle constraint respectively. We

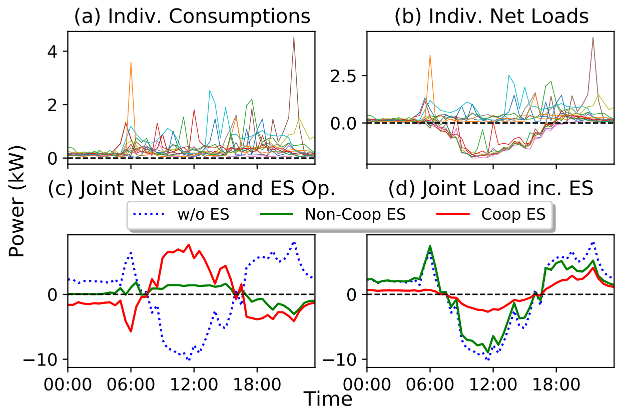

Fig. 1. 14 Prosumer loads: (a) individual load consumption, (b) individual load including PV generation, (c) grand coalition load and non-cooperative and cooperative ES operation profiles, (d) grand coalition load with non-cooperative and cooperative ES operation.

consider each prosumer i's ES system has an *energy capacity* (kWh) of $e_i \geq 0$, a *charge limit* (kWh) of $\overline{b}_i \geq 0$ and a *discharge limit* (kWh) of $\underline{b}_i \geq 0$ over the time span of Δt, a *charge efficiency* of $\eta_i^{in} \in (0,1)$ and a *discharge efficiency* of $\eta_i^{out} \in (0,1)$, an upper *state of charge* limit of $\overline{SoC}_i \in [0,1]$ and a lower *state of charge* limit of $\underline{SoC}_i \in [0,1]$, and an *initial state of charge* of $SoC_i^0 \in [0,1]$. For a prosumer who does not own an ES system, we set their energy capacity and charge/discharge limits all as zeros.

It is understood that the ES systems degrade with usage. In order to obtain the accurate ES inputs, it needs to undergo regular reference performance tests, which cost time and introduce additional degradation [28]. To reduce the cost and time, a data-driven state of health estimation method is introduced in [29], which has the potential to be implemented if the concern for privacy violation could be mitigated.

Fig. 1 demonstrates the effect of cooperative ES operation in a 14-prosumer scenario. As shown in (d), the cooperative ES operation tends to flatten the load as it tries to match the consumption and generation within the coalition to minimize the *coalition energy cost*.

2.2. Value of coalitions

The purpose of using cooperative game theory is to establish a framework to quantify the benefit of cooperation, and then to allocate the benefit to the participants efficiently. The *coalitional energy cost* provides a great metric to evaluate a coalition's performance. Here, we define the value of a coalition $\mathcal{T}$ as the energy cost savings obtained by forming the coalition. This is given by the difference between the sum of the energy costs of all the prosumers in $\mathcal{T}$ when they schedule the ES systems individually, and the minimum *coalitional energy cost* of $\mathcal{T}$ when the prosumers schedule their ES systems collectively: $v(\mathcal{T}) = \sum_{i\in\mathcal{T}} G(\{i\}) - G(\mathcal{T})$.

By this definition, the value of the *grand coalition* becomes the total energy cost savings of a P2P cooperative game, which denotes the total amount of payoffs we can award to all the participants.

2.3. Prosumer payoffs and shapley value

The second step in a cooperative game framework is the allocation of payoffs. We use vector $\mathbf{x} \in \mathbb{R}^N$ as the *payoff allocation* whose entry x_i represents the payment to prosumer $i \in \mathcal{N}$. One important payoff allocation is called the Shapley value denoted as $\phi = \{\phi_i, \forall i \in \mathcal{N}\}$ [24], representing each player's weighted average marginal contribution to all possible coalitions within the game:

$$\phi_i = \sum_{\mathcal{T}\subset\mathcal{N}, i\notin\mathcal{T}} \frac{(|\mathcal{T}|)!(N-|\mathcal{T}|-1)!}{N!}[v(\mathcal{T}\cup i) - v(\mathcal{T})]. \quad (4)$$

The Shapley value also satisfies the following axioms:

1) (*Efficiency*) $\sum_{i\in\mathcal{N}} \phi_i = v(\mathcal{N})$. This requires the entirety of the value created by the *grand coalition* to be allocated to the players.
2) (*Individual Rationality*) $\phi_i \geq v(\{i\}), \forall i \in \mathcal{N}$. This ensures that no player is penalized for cooperating.
3) (*Symmetry*) If $v(\mathcal{T}\cup\{i\}) = v(\mathcal{T}\cup\{j\}), \forall \mathcal{T} \subseteq \mathcal{N}, \mathcal{T}\cap\{i,j\} = \emptyset$, then $\phi_i = \phi_j$. This means that two players should be assigned the same Shapley value if they have the same marginal contributions to all the coalitions.
4) (*Dummy Axiom*) If $v(\mathcal{T}) = v(\mathcal{T}\cup\{i\}), \forall \mathcal{T} \subseteq \mathcal{N}, \mathcal{T}\cap\{i\} = \emptyset$, then $\phi_i = 0$. Therefore, a player's Shapley value should be zero if they add zero marginal value to any of the coalitions.
5) (*Additivity*) If v and u are characteristic functions, then $\phi_i(v+u) = \phi_i(v) + \phi_i(u), \forall i \in \mathcal{N}$. This indicates that the Shapley value of two games played at the same time should be the sum of the two games' Shapley values when played separately.

Axiom (1) guarantees that all the profits allocated to the prosumers add up to the total energy cost savings from the *grand coalition*. In our P2P cooperative game, $v(\{i\}) = 0, \forall i \in \mathcal{N}$, so Axiom (2) requires $\phi_i \geq 0, \forall i \in \mathcal{N}$. Axiom (3) and (4) indicate the *'fairness'* of the payoff allocation. Axiom (5) is not actively used in this paper as the P2P cooperative game is the only game discussed.

The Shapley value offers a way to incentivize prosumers to participate in this cooperative scheme, improving the local energy supply reliability while encouraging the efficient use of distributed renewable generation. However, the scalability of the proposed model is very limited because the Shapley value's computational time increases exponentially with the size of the grand coalition. The following section looks into a sampling method to estimate the Shapley value to reduce the model's computational complexity.

3. ESTIMATION OF SHAPLEY VALUE

The scalability of the P2P cooperative game model is mainly limited by the sheer number of cost minimization problems that are required to be solved. This number is equal to the number of possible coalitions 2^N, where N is the number of participating prosumers. Since the Shapley value is the weighted average of a player's marginal contributions, sampling is identified as a promising estimation technique to be applied in our P2P cooperative game.

3.1. Stratified random sampling

The conventional definition is expressed in (4). [30] provided an alternative definition of the Shapley value expressed in terms of all possible orders of the players, which was then adopted by [26] to develop a random sampling method to estimate the Shapley value. In this approach, $\pi(\mathcal{N})$ is defined as the set of all possible permutations with player set $\mathcal{N}$, where each permutation is a sequence of all the players in a specific order. For a given permutation $O \in \pi(\mathcal{N})$, $O(l)$ denotes the player in position l, and $Pre^i(O)$ denotes the set of predecessors of Player i, or the coalition of players that are positioned ahead of Player i in the player sequence represented by O. Therefore, if $i = O(l)$, $Pre^i(O) = \{O(1), O(2), ..., O(l-1)\}$. Player i's marginal contribution to the coalition $Pre^i(O)$ is thus a function of O:

$$\delta(O)_i = v(Pre^i(O) \cup i) - v(Pre^i(O)). \tag{5}$$

The alternative definition of the Shapley value can be written as

$$\phi_i = \sum_{O \in \pi(\mathcal{N})} \frac{1}{N!}\delta(O)_i, \ \ i \in \mathcal{N}. \tag{6}$$

Since $|\pi(\mathcal{N})| = N!$ and $\delta(O)_i$ are equally weighted for all $O \in \pi(\mathcal{N})$ in (6), the Shapley value can be estimated using the unweighted expectation of $\delta(O)_i$ given a set of randomly sampled permutations M:

$$\phi_i = \sum_{O \in M} \frac{1}{|M|}\delta(O)_i, \ \ i \in \mathcal{N}. \tag{7}$$

Notice that when $M = \pi(\mathcal{N})$, (7) becomes the Shapley value's alternative definition in (6).

Using (7), the Shapley value can be estimated from randomly sampling player permutations [26]. To improve the estimation accuracy, [27] proposed a stratified random sampling approach to divide the population of all player permutations into subpopulations that have the same size of predecessors for each player. This stratified random sampling method follows the following steps.

1) A stratum, or a stratified set of player permutations is defined as $P_{il} := \{O \in \pi(\mathcal{N}) \mid O(l) = i, \forall i, l \in [1, N]\}$. Therefore, P_{il} contains every permutation $O \in \pi(\mathcal{N})$, in which player i is in position l. Player i's mean marginal contribution of each stratum is

$$\phi_{il} = \frac{1}{|P_{il}|} \sum_{O \in P_{il}} \delta(O)_i, \ \ \forall i, l \in [1, N]. \tag{8}$$

2) A random permutation sample M_{il} of size $|M_{il}|$ is obtained with replacement from each stratum P_{il}.
3) Adapted from (8), player i's mean marginal contribution of the samples from each stratum is

$$\overline{\phi}_{il} = \frac{1}{|M_{il}|} \sum_{O \in M_{il}} \delta(O)_i, \ \ \forall i, l \in [1, N]. \tag{9}$$

The estimated Shapley value can then be calculated as $\hat{\phi}_i^{st} = \sum_{l=1}^{N} \frac{1}{N}\overline{\phi}_{il}$, $\forall i \in [1, N]$.

3.2. Modified sampling with optimal sample allocation

We notice that in (9), $\delta(O)_i$ are equally weighted for all $O \in M_{il}$. Because each player set (coalition) $Pre^i(O)$ appears $(l-1)!(N-l)!$ times for a given l, they have the same probability of being sampled from P_{il} into M_{il}. We define the *coalitional stratum* as the set of coalitions $Q_{il} := \{\mathcal{T} \subseteq \mathcal{N} \mid i \notin \mathcal{T}, |\mathcal{T}| = l-1, \forall i, l \in [1, N]\}$, and $\Delta(\mathcal{T})_i = v(\mathcal{T} \cup i) - v(\mathcal{T})$. We then obtain a random sample H_{il} with replacement from Q_{il}, and because the order of players does not matter in a coalition, H_{il} can be considered a combination sample. Equation (9) can be rewritten as

$$\overline{\phi}_{il} = \frac{1}{|H_{il}|} \sum_{\mathcal{T} \in H_{il}} \Delta(\mathcal{T})_i, \ \ \forall i, l \in [1, N]. \tag{10}$$

In order to implement the stratified random sampling method, a procedure to determine the sample size of each stratum needs to be established. [26] identified the true variance as a metric to allocate the samples among strata to minimize the estimation error, and proposed a two-stage Shapley value estimation algorithm with optimal sample allocation. In the first stage, 50% of the samples are evenly distributed to each stratum to obtain an initial estimated Shapley value and each stratum's sample variance. In the second stage, the remaining 50% of the samples are optimally allocated to each stratum in proportion to their sample variances calculated in the first stage. The final estimated Shapley value is then calculated using the sampling results from both stages.

We then recognize that $|Q_{il}| = \frac{(N-1)!}{(l-1)!(N-l)!}$, which means that evenly dividing the samples in the first stage could result in a sample size larger than the size of some *coalitional strata*: $|H_{il}| > |Q_{il}|$, especially when l is close to 1 or N. For these *coalitional strata*, calculating the accurate mean marginal contribution ϕ_{il} requires less samples than its estimate $\overline{\phi}_{il}$ with random sampling:

$$\phi_{il} = \frac{1}{|Q_{il}|} \sum_{\mathcal{T} \in Q_{il}} \Delta(\mathcal{T})_i, \ \ \forall i, l \in [1, N]. \tag{11}$$

With (10) and (11), the modified two-stage stratified random sampling method with optimal sample allocation is detailed in Algorithm 1.

For the basic coalitional stratified random sampling with optimal sample allocation, the main input is the total sample size h, and the main output is the estimated Shapley value $\hat{\phi}$. Stratum parameters $\boldsymbol{\Phi} = \{\Phi_{il}\}, \boldsymbol{s} = \{s_{il}\}, \forall i, l \in [1, N]$ are updated throughout the process to facilitate the computation of the sample variances $\overline{\sigma}^2_{il}$ and the mean marginal contributions $\overline{\phi}_{il}$ for each coalitional stratum. $\boldsymbol{h} = \{h_{il}\}, \forall i, l \in [1, N]$ denotes the total number of samples taken for each coalitional stratum. If the algorithm is implemented on its own without any preceding sampling steps, we initiate the algorithm by setting $\boldsymbol{\Phi}' = \mathbf{0}, \boldsymbol{s}' = \mathbf{0}, \boldsymbol{h}' = \mathbf{0}$. After the algorithm is implemented, the output $\boldsymbol{\Phi}'', \boldsymbol{s}'', \boldsymbol{h}''$ store the updated values. These three parameters are important for the multi-step sampling explained in Section 3.3.

In Stage A, if the evenly distributed sample size is bigger than the stratum size: $h^A_{il} > |Q_{il}|$, we compute the prosumer's marginal contribution in all the possible samples in this coalitional stratum by setting $H^A_{il} \leftarrow Q_{il}$, $h^{tot}_{il} \leftarrow |Q_{il}|$. The precise mean marginal contribution of Q_{il} can thus be obtained: $\phi_{il} = \overline{\phi}_{il}$. Meanwhile, the saved samples $h^A_{il} - |Q_{il}|$ can be added to Stage B. This way, The number of samples remains the same to maintain a similar computation time, while the accuracy of the estimation is improved with the precise stratum marginal contribution for some strata, and an increased number of samples for the optimal allocation.

Algorithm 1: Coalitional Stratified Random Sampling with Optimal Sample Allocation (inputs: $h, \boldsymbol{\Phi}', \boldsymbol{s}', \boldsymbol{h}'$).

Stage A
$\boldsymbol{\Phi} \leftarrow \boldsymbol{\Phi}'$, $\boldsymbol{s} \leftarrow \boldsymbol{s}'$
$h^A_{il} \leftarrow \frac{h}{2N^2}$
$\Omega \leftarrow \varnothing$: set of strata with sample sizes determined
for $i \in [1,N], l \in [1,N]$ **do**
  if $h^A_{il} > |Q_{il}| = \frac{(N-1)!}{(l-1)!(N-l)!}$ **then**
    $H^A_{il} \leftarrow Q_{il}$, $h^{tot}_{il} \leftarrow |Q_{il}|$
    $h \leftarrow h - |Q_{il}|$, $\Omega \leftarrow \Omega \cup (i,l)$
  else
    $H^A_{il} \leftarrow h^A_{il}$ samples with replacement from Q_{il}
  for $\mathcal{T} \in H^A_{il}$ **do**
    $\Delta(\mathcal{T})_i = v(\mathcal{T} \cup i) - v(\mathcal{T})$
    $\Phi_{il} \leftarrow \Phi_{il} + \Delta(\mathcal{T})_i$, $s_{il} \leftarrow s_{il} + (\Delta(\mathcal{T})_i)^2$
  $\overline{\sigma}^2_{il} \leftarrow \frac{1}{h^0_{il}+|H^A_{il}|-1}(s_{il} - \frac{(\Phi_{il})^2}{h^0_{il}+}|H^A_{il}|)$

Stage B
$\omega \leftarrow \{(0,0)\}$: initialize ω to start following **while** loop
while $\omega \neq \varnothing$ **do**
  for $i \in [1,N], l \in [1,N]$ **and** $(i,l) \notin \Omega$ **do**
    $h^{tot}_{il} \leftarrow h \frac{\overline{\sigma}^2_{il}}{\sum_{i=1}^{N} \sum_{l=1}^{N} \overline{\sigma}^2_{il}}$
    $h^B_{il} \leftarrow h^{tot}_{il} - h^A_{il}$
  $\omega \leftarrow \varnothing$: set of over-sampled strata in **Stage 1**
  for $i \in [1,N], l \in [1,N]$ **and** $(i,l) \notin \Omega$ **do**
    if $h^B_{il} < 0$ **then**
      $h^{tot}_{il} \leftarrow h^A_{il}$, $h \leftarrow h - h^A_{il}$, $\omega \leftarrow \omega \cup (i,l)$
  $\Omega \leftarrow \Omega \cup \omega$
for $i \in [1,N], l \in [1,N]$ **and** $(i,l) \notin \Omega$ **do**
  $H^B_{il} \leftarrow h^B_{il}$ samples with replacement from Q_{il}
  for $\mathcal{T} \in H^B_{il}$ **do**
    $\Phi_{il} \leftarrow \Phi_{il} + \Delta(\mathcal{T})_i$, $s_{il} \leftarrow s_{il} + (\Delta(\mathcal{T})_i)^2$
for $i \in [1,N]$ **do**
  for $l \in [1,N]$ **do**
    $h^{tot}_{il} \leftarrow h^{tot}_{il} + h^0_{il}$
    $\overline{\phi}_{il} \leftarrow \frac{\Phi_{il}}{h^{tot}_{il}}$
  $\hat{\phi}^{st,opt}_i \leftarrow \sum_{l=1}^{N} \frac{1}{N} \overline{\phi}_{il}$
$\boldsymbol{\Phi}'' \leftarrow \{\Phi_{il}\}, \boldsymbol{h}'' \leftarrow \{h^{tot}_{il}\}, \forall i, l \in [1,N]$, $\boldsymbol{s}'' \leftarrow \boldsymbol{s}$
$\hat{\phi} \leftarrow \{\hat{\phi}^{st,opt}_i\}, i \in [1,N]$
return $\hat{\phi}, \boldsymbol{\Phi}'', \boldsymbol{s}'', \boldsymbol{h}''$

3.3. Multi-step sampling

Regardless of the sampling method, one common input in these estimation models is the total sample size. It is intuitive that the higher the sample size is, the more accurate the estimation results tend to be, but the longer the model is going to take. Considering that the goal of the estimation is to scale up the game while maintaining a reasonably accurate estimation of the Shapley value, the two main metrics to evaluate the performance of an estimation method should be the computation time τ and the estimation accuracy, measured by the *standard error of the estimate* as a percentage of the average player payoff:

$$\frac{\sigma(\hat{\mathbf{x}}, \mathbf{x})}{\overline{x}} = \frac{\sqrt{\sum_i^N (\hat{x}_i - x_i)^2 / N}}{v(\mathcal{N})/N} \times 100\%, \tag{12}$$

where $\hat{\mathbf{x}}$, $\mathbf{x}$, and $\overline{x}$ represent the estimated, the benchmark, and the average payoffs respectively.

For a game of a small number of players, the estimation accuracy can be evaluated by comparing the results to those from the full Shapley value calculation. However, a large number of tests with different sample sizes may be needed to identify the minimum sample size h^* required to achieve a certain level of estimation accuracy $\sigma^*/\overline{x}$. Additionally, for games of different sizes, and even for games of the same size but of different prosumer compositions, h^* might be different. It thus becomes computationally cumbersome to have to identify h^* for every new game. For a game of a size too large to compute the true Shapley

Algorithm 2: Multi-Step Coalitional Stratified Random Sampling with Optimal Sample Allocation (inputs: h, W, σ^*).

$\rho \leftarrow h/U$
$\boldsymbol{\Phi}^0 \leftarrow \mathbf{0},\ \boldsymbol{s}^0 \leftarrow \mathbf{0},\ \boldsymbol{h}^0 \leftarrow \mathbf{0}, \hat{\phi}^0 \leftarrow \mathbf{0}$
for $u \in [1, U]$ **do**
  $(\hat{\phi}^u, \boldsymbol{\Phi}^u, \boldsymbol{s}^u, \boldsymbol{h}^u) \leftarrow W(\rho, \boldsymbol{\Phi}^{u-1}, \boldsymbol{s}^{u-1}, \boldsymbol{h}^{u-1})$
  if $\sigma(\hat{\phi}^u, \hat{\phi}^{u-1}) \leq \sigma^*$ **then**
    end for loop.
$\hat{\phi} \leftarrow \hat{\phi}^u$
$h^* \leftarrow \rho u$
return $\hat{\phi}, h^*$

value, directly measuring the estimation accuracy is simply infeasible.

To address the challenge of sample size selection, a multi-step sampling strategy is proposed in this paper. In this strategy, we consider h as the maximum sample size, and the sampling process is divided into U steps, with each step of sample size $\rho = h/U$. We use functional W to represent Algorithm 1: $(\hat{\phi}, \boldsymbol{\Phi}'', \boldsymbol{s}'', \boldsymbol{h}'') = W(h, \boldsymbol{\Phi}', \boldsymbol{s}', \boldsymbol{h}')$. And the implementation of the multi-step sampling strategy is presented in Algorithm 2.

The main idea of the multi-step strategy is to verify the estimation results as the the sampling process proceeds. The sampling results are stored in memory, and as more samples are added in each sampling step, the Shapley value estimation is updated based on the results in all previous steps. After each step is completed, the updated estimation results are compared against those of the last step, and if the estimation difference between the two steps measured by the *standard error* is below the set threshold: $\sigma(\hat{\phi}^u, \hat{\phi}^{u-1}) \leq \sigma^*$, the algorithm stops as it is considered that the estimation $\hat{\phi} = \hat{\phi}^u$ has reached the desired accuracy. At this point, if the total number of samples drawn is less than the set maximum sample size: $h^* < h$, additional computation time is saved than the basic coalitional stratified random sampling. Note that in order to obtain the actual *standard error of the estimate* of the Shapley value $\sigma(\hat{\phi}^u, \phi)$, the true Shapley value ϕ needs to be computed. It is computationally intractable for larger games, but the case study in Section 4.1 shows a small game of 20 players to validate the effectiveness of this proposed multi-step sampling strategy.

4. CASE STUDIES

In the following three case studies, we implement the proposed sampling method to estimate the Shapley value of the P2P cooperative game. In the first case study, we select a range of prosumer numbers so we can compare the estimation accuracies and computation times of the Shapley value estimation methods and the full Shapley value calculation. In the second case study, we focus on the potential financial losses for an individual player caused by stochastic error, battery degradation, and the Shapley value estimation error, and compare these losses with their financial benefit gained from the game. In the third case study, we scale up the size of the game to evaluate the payoffs to the prosumers based on their DER types.

Some of the model inputs are as follows: the domestic load data was measured in the Customer-Led Network Revolution trials[1]. the model time frame is 24 hours starting from the midnight of a sunny summer day in July. The PV systems are 4kW with fixed 20 degree tilt, simulated in PVWatts[2] using the London Gatwick solar data. The ES model has an *energy capacity* of 7 kWh, a maximum charge power of 3.5 kW, a maximum discharge power of 3.2 kW, both charge and discharge efficiencies of 95%, an *initial state of charge* of 50%, and a *state of charge* range of 20-95%. The energy import price follows a UK Economy 7 residential rate structure: £0.08/kWh for midnight-7am, and £0.18/kWh for 7am-midnight[3], and the energy export price is the UK feed-in tariff[4] fixed at £0.0379/kWh.

4.1. Sampling-based shapley estimation validation

In this case study, we focus on a 14-player game, for which the true Shapley value can be easily computed. The PV and ES adoption rates are both fixed at 50%, and both ownerships are randomly assigned independently of each other. In other words, each prosumer can have a PV system, or an ES system, or both, or neither. We apply the proposed multi-step sampling technique to both the random sampling method and the modified stratified sampling. Using $h = 2000N$, $U = 20$, we record the Shapley value estimation at the end of each step $\hat{\phi}^u$, and the estimation difference between every two steps measured by the *standard error* $\sigma(\hat{\phi}^u, \hat{\phi}^{u-1})$. We then compare $\hat{\phi}^u$ with the true Shapley value ϕ to verify its accuracy by calculating its *standard error of the estimate* $\sigma(\hat{\phi}^u, \phi)$. The model is run for 30 different games, each with randomly selected load profiles and PV, ES assignments.

The results are shown in Fig. 2 with the standard error for each step averaged over 30 runs. Each data point on a dotted line represents the standard error between the estimations of the current step and the previous step. Each data point on a solid line represents the standard error between the estimation of the current step and the true Shapley value. The random sampling method and the modified stratified sampling method are represented by yellow and blue lines respectively. It can be seen that

[1] www.networkrevolution.co.uk/project-library/dataset-tc5-enhanced-profiling-solar-photovoltaic-pv-users/
[2] pvwatts.nrel.gov/pvwatts.php
[3] www.gov.uk/government/collections/domestic-energy-prices
[4] www.ofgem.gov.uk/environmental-programmes/fit/fit-tariff-rates

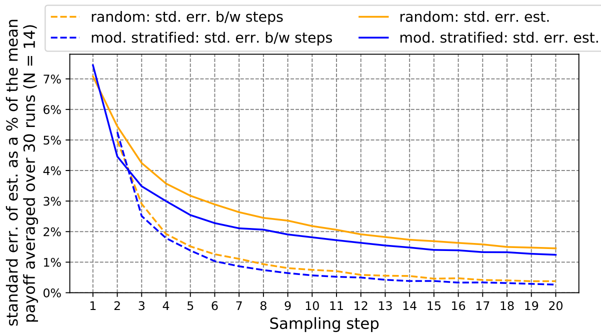

Fig. 2. Standard error comparison using the multi-step sampling technique: random sampling vs. stratified sampling (N= 14). The data for each sampling method at each sampling step are averaged over 30 runs with different inputs of prosumer load and DER ownerships.

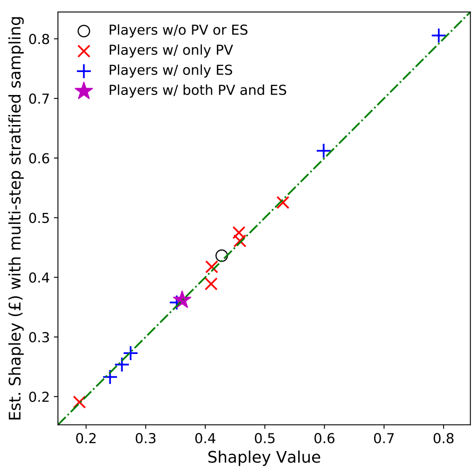

Fig. 3. True Shapley value vs. estimated Shapley values using multi-step stratified sampling (N= 14).

$\sigma(\hat{\phi}^u, \hat{\phi}^{u-1})$ for both methods follow a similar declining trajectory, while the stratified sampling method consistently produces more accurate estimates of the Shapley value as more samples are drawn. For example, it takes only 7 steps for the stratified sampling method to produce an estimate that has a 2% standard error from the true Shapley value ($\sigma(\hat{\phi}^u, \phi) \approx 2\%$), whereas the basic random sampling method requires 11 steps to reach the same accuracy. We also notice that $\sigma(\hat{\phi}^u, \phi)$ stops showing significant improvement after Step 7, which is around the time when $\sigma(\hat{\phi}^u, \hat{\phi}^{u-1})$ reaches 1%. Therefore, we choose $\sigma^* = 1\% \times \bar{x}$ as the estimation accuracy criterion for the remaining case studies. A comparison of the true Shapley value and the multi-step sampling estimation for each player in this 14-player game is shown in Fig. 3. It further demonstrates that regardless of the player type, the estimated values closely resemble the true Shapley value.

Applying Algorithm 2, we are able to scale up the game to 100 players within a reasonable time. Table 1 shows the 10-run average computation time[5] of the three models. We consider any time above 10 hours to be impractical for this application. As predicted, the full Shapley value calculation is shown to be intractable. Sampling is able to scale up the game significantly, and the proposed multi-step sampling method can even compute the estimated Shapley value in 1 hour for a 100-player game.

Table 1. Model Computation Time τ (s).

No. players	10	14	20	50	100
full model	2E+1	3E+2	2E+4	N/A*	N/A
full sampling	2E+1	2E+2	1E+3	4E+3	2E+4
multi-step smpl	2E+1	1E+2	3E+2	9E+2	4E+3

* N/A means the computation takes longer than 10 hours.

4.2. Single prosumer payoff analysis

This case study focuses on the financial payoff for an individual prosumer. Still using the 14-player game shown in Fig. 3 as an example, we focus on the only player that owns both PV and ES (marked by ★), and conduct a worst-case scenario analysis. Using the estimated Shapley value, this player receives a reward of £0.36.

First, we consider the ES degradation cost, which is not directly built into the cooperative game theoretic model mainly due to the short time frame (24 hours). The average wear cost (AWC) calculation presented in [31] is used to estimate the cost incurred by the cooperation:

$$AWC = \frac{\text{Battery Price}}{ACC(DoD) \times 2 \times DoD \times e \times \eta^{in} \times \eta^{out}}, \quad (13)$$

where DoD is the depth of discharge, and ACC is the achievable cycle count, a function of DoD. Based on the model inputs, we have $e = 7kWh$, $\eta^{in} = \eta^{out} = 95\%$ and a *state of charge* range of 20-95%. Assuming the ES unit in the model is a battery with a unit price of \$156/kWh[6], the battery costs around £850 with a year 2019 average conversion rate of $£1 = \$1.28$[7]. Using a conservative 80% DoD, we have $ACC(80\%) = 1000$ based on [32]. Therefore, it can be calculated for this player that $AWC \approx £0.084$/kWh. The player's battery operation profiles with and without cooperation are shown in Fig. 4, which yields an additional 0.31kWh round-trip operation for the cooperative case. Therefore, the wear cost incurred by the cooperative scheme is $£0.084 \times 0.31 = £0.026$, equivalent to 7.24% of the original reward.

Second, we analyze the impact of stochastic errors on the prosumer financial payback. We conduct a Monte

[5] Running on a computer equipped with 16 GB RAM and a 2.8 GHz Quad-Core Intel Core i5 processor.
[6] https://about.bnef.com/blog/battery-pack-prices-fall-as-market-ramps-up-with-market-average-at-156-kwh-in-2019/
[7] https://www.macrotrends.net/2549/pound-dollar-exchange-rate-historical-chart

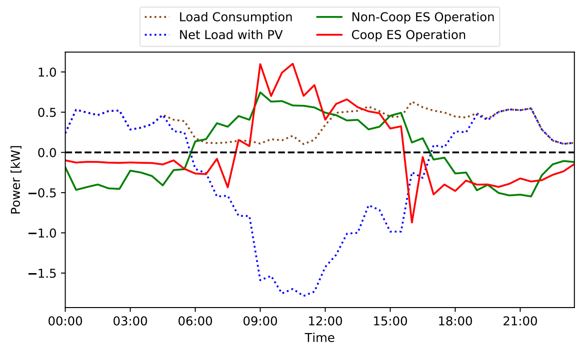

Fig. 4. Energy profiles of a player with both PV and ES in a 14-player game.

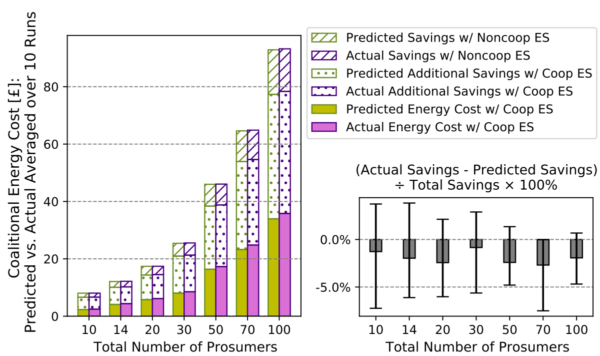

Fig. 5. The impact of stochastic errors on the grand coalition energy cost savings.

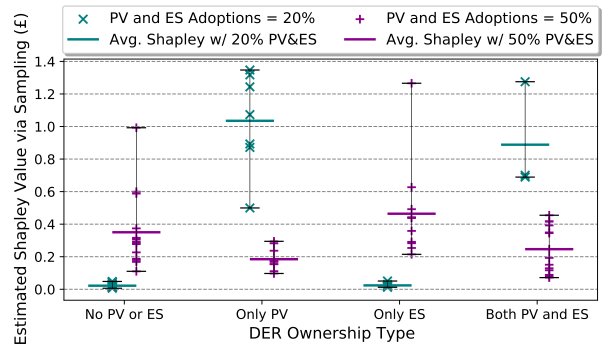

Fig. 6. Estimated Shapley value by DER ownership type with two different DER adoption rates (20% vs. 50%).

Carlo analysis by treating all input load and PV profiles as predictions. The actual load and PV profiles are generated assuming the value for each time step follows a normal distribution, for which the mean value is equal to the predicted value and the standard deviation can be specified. The actual coalitional energy cost savings is calculated by applying to the actual profiles the ES operations optimized based on the predicted profiles. Assuming a standard deviation of 5% for solar, and 15% for prosumer loads, the model is run 10 times for games of each size, which ranges from 10 to 100 players. The results are shown in Fig. 5. For all the tested cases, the saving reduction is all less than 10% of the total savings, which can be distributed in proportion to the player payoffs. We consider the worst case for the player in this case is a 10% payoff reduction.

Last, based on Fig. 2, the Shapley estimation can introduce around 2% error, which is another 2% payoff reduction in the worst case. In total, the worst case can amount to a total of roughly 20% reduction of payoff, which still leaves a profit of £$0.36 \times 80\% =$ £0.29 for the player.

4.3. Sampling-based shapley estimation for large games

Having demonstrated the effectiveness of the Sampling methods in estimating the Shapley value, we can now investigate the impact of various inputs on the model results for large games. For a P2P cooperative game with 50 prosumers, Fig. 6 compares the estimated Shapley values by players' DER ownership type, where each marker represents a prosumer's estimated Shapley value. There are a few interesting observations. First, except for a few outliers, prosumers with the same DER ownership type are rewarded similar Shapley values regardless of the overall DER adoption rate. Second, as the DER adoption rates change, there is a significant shift in the Shapley values; when the DER adoption rates are low, PV owners are awarded significantly higher Shapley values likely because they provide cheaper energy to the coalitions, while when the DER adoption rates are high, pure consumers and ES owners are awarded higher Shapley values likely because they absorb more local generation. Third, as the DER adoption rates increase, the average Shapley values by DER ownership type tends to converge despite the wider spread among the pure consumers and prosumers with only ES systems.

With the same 50 prosumers, we then pick out four typical prosumers with different DER ownership types, and run the P2P cooperative model under four different scenarios: 1) PV adoption rate is fixed at 30%, and ES adoption rate varies from 10% to 50%, 2) PV adoption rate is fixed at 50%, and ES adoption rate varies from 10% to 50%, 3) ES adoption is rate fixed at 30%, and PV adoption rate varies from 10% to 50%, and 4) PV and ES are with the same adoption rate that varies from 10% to 50%. Fig. 7 illustrates how the Shapley value changes with different DER adoption rates. Based on the DER ownership type, the trend at which the Shapley value changes with the varying DER adoption rates can be very different. For example, a consumer that does not own any PV or ES tends to be awarded more when the adoption rates for the PV and ES increase together, whereas a prosumer that owns both PV and ES display the opposite trend. It is interesting to note that when the PV adoption rate is fixed, whether at 30% or 50%, varying the ES adoption rate has very little influence on the Shapley value regardless of the prosumer type. In contrast, whether the ES adoption rate is

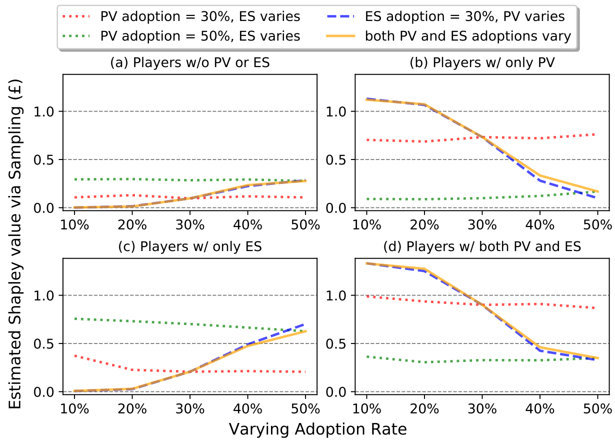

Fig. 7. Estimated Shapley value with varying PV and ES adoption rates.

fixed at 30% or follows the PV adoption rate, varying the PV adoption rate has a significant impact on the Shapley value of all prosumer types.

It is worth noting that the main purpose of the case studies is to validate the scalability of the proposed sampling method applied in the P2P cooperative game. The specific results shown are dependent on the assumptions made about the PV, ES system specifications, and the energy prices. Further sensitivity analyses are required to generalize the results to other markets.

5. CONCLUSION

To improve the scalability of a cooperative game based P2P market, this paper proposes the novel application of a coalitional stratified random sampling method to estimate the Shapley value. A multi-step sampling approach is created to divide the sampling process to smaller steps. By measuring the standard error of the estimate between steps, it provides a way to verify the estimation results and terminates the sampling process once a certain estimation accuracy threshold is achieved, further reducing the computation time. The maximum size of the game that can be computed in a reasonable time (< 10 hours) is thus increased from less than 20 players to over 100 players. For games that are small enough to generate the true Shapley value, the effectiveness of the proposed method is demonstrated by showing a standard error of the estimate smaller than 2% of a player's average payoff. The proposed model is then run on a P2P cooperative game of 50 players to demonstrate the patterns of the Shapley value for different prosumer DER ownership types and with varying DER adoption rates. It shows that compared to the ES adoption rate, the PV adoption rate has a much larger impact, both negative and positive depending on the DER ownership type, on the prosumer payoffs.

REFERENCES

[1] J. Skea, D. Anderson, T. Green, R. Gross, P. Heptonstall, and M. Leach, "Intermittent renewable generation and the cost of maintaining power system reliability," *IET Gener. Transm. Distrib.*, vol. 1, no. 2, p. 324, 2007.

[2] H. K. Jacobsen and S. T. Schroder, "Curtailment of renewable generation: Economic optimality and incentives," *Energy Policy*, vol. 49, pp. 663-675, 2012.

[3] K. Worthmann, C. M. Kellett, P. Braun, L. Grüne, and S. R. Weller, "Distributed and decentralized control of residential energy systems incorporating battery storage," *IEEE Trans. on Smart Grid*, vol. 6, pp. 1914-1923, Jul. 2015.

[4] D. F. Zhang, S. P. Zhang, Z. Q. Wang, and B. C. Lu, "Dynamic control allocation algorithm for a class of distributed control systems," *International Journal of Control, Automation and Systems*, vol. 18, no. 2, pp. 259-270, 2020.

[5] T. Morstyn, B. Hredzak, R. P. Aguilera, and V. G. Agelidis, "Model predictive control for distributed microgrid battery energy storage systems," *IEEE Trans. on Control Systems Technology*, vol. 26, pp. 1107-1114, May 2018.

[6] Y. Parag and B. K. Sovacool, "Electricity market design for the prosumer era," *Nature Energy*, vol. 1, p. 16032, March 2016.

[7] T. Sousa, T. Soares, P. Pinson, F. Moret, T. Baroche, and E. Sorin, "Peer-to-peer and community-based markets: A comprehensive review," *Renewable and Sustainable Energy Reviews*, vol. 104, pp. 367-378, March 2019.

[8] I. A. Sajjad, G. Chicco, and R. Napoli, "Definitions of demand flexibility for aggregate residential loads," *IEEE Trans. on Smart Grid*, vol. 7, pp. 2633-2643, Nov 2016.

[9] A. Pyrgou, A. Kylili, and P. A. Fokaides, "The future of the feed-in tariff (fit) scheme in europe: The case of photovoltaics," *Energy Policy*, vol. 95, pp. 94-102, 2016.

[10] N. Martin and J. Rice, "Solar feed-in tariffs: Examining fair and reasonable retail rates using cost avoidance estimates," *Energy Policy*, vol. 112, pp. 19-28, 2018.

[11] D. Kalathil, C. Wu, K. Poolla, and P. Varaiya, "The sharing economy for the electricity storage," *IEEE Trans. on Smart Grid*, vol. 10, pp. 556-567, Jan 2019.

[12] Y. Zhou, J. Wu, and C. Long, "Evaluation of peer-to-peer energy sharing mechanisms based on a multiagent simulation framework," *Applied Energy*, vol. 222, pp. 993-1022, February 2018.

[13] L. Jia and L. Tong, "Dynamic pricing and distributed energy management for demand response," *IEEE Trans. on Smart Grid*, vol. 7, pp. 1128-1136, March 2016.

[14] N. Liu, X. Yu, C. Wang, and J. Wang, "Energy sharing management for microgrids with pv prosumers: A stackelberg game approach," *IEEE Trans. on Industrial Informatics*, vol. 13, pp. 1088-1098, June 2017.

[15] B. Zhang, C. Jiang, J. L. Yu, and Z. Han, "A contract game for direct energy trading in smart grid," *IEEE Trans. on Smart Grid*, vol. 9, pp. 2873-2884, July 2018.

[16] J. Lee, J. Guo, J. K. Choi, and M. Zukerman, "Distributed energy trading in microgrids: A game-theoretic model and its equilibrium analysis," *IEEE Trans. on Industrial Electronics*, vol. 62, pp. 3524-3533, June 2015.

[17] Y. Zhang, S. Liang, and H. Ji, "Distributed Nash equilibrium seeking for aggregative games via derivative feedback," *International Journal of Control, Automation and Systems*, vol. 18, no. 5, pp. 1075-1082, 2020.

[18] J. L. Zhang, D. L. Qi, and M. Yu, "A game theoretic approach for the distributed control of multi-agent systems under directed and time-varying topology," *International Journal of Control, Automation and Systems*, vol. 12, no. 4, pp. 749-758, 2014.

[19] L. Han, T. Morstyn, and M. McCulloch, "Incentivizing prosumer coalitions with energy management using cooperative game theory," *IEEE Trans. on Power Systems*, vol. 34, pp. 303-313, Jan 2019.

[20] W. Lee, L. Xiang, R. Schober, and V. W. S. Wong, "Direct electricity trading in smart grid: A coalitional game analysis," *IEEE Journal on Selected Areas in Communications*, vol. 32, no. 7, pp. 1398-1411, 2014.

[21] P. Chakraborty, E. Baeyens, K. Poolla, P. P. Khargonekar, and P. Varaiya, "Sharing storage in a smart grid: A coalitional game approach," *IEEE Trans. on Smart Grid*, vol. 10, pp. 4379-4390, July 2019.

[22] C. Feng, F. Wen, S. You, Z. Li, F. Shahnia, and M. Shahidehpour, "Coalitional game-based transactive energy management in local energy communities," *IEEE Trans. on Power Systems*, vol. 35, pp. 1729-1740, May 2020.

[23] L. Han, T. Morstyn, and M. McCulloch, "Constructing prosumer coalitions for energy cost savings using cooperative game theory," *Proc. of Power Systems Computation Conference (PSCC)*, pp. 1-7, June 2018.

[24] L. S. Shapley, "Cores of convex games," *International Journal of Game Theory*, vol. 1, no. 1, pp. 11-26, 1971.

[25] A. C. Chapman, S. Mhanna, and G. Verbič, "Cooperative game theory for non-linear pricing of load-side distribution network support," *Proc. of The 3rd IJCAI Algorithmic Game Theory Workshop*, 2017.

[26] J. Castro, D. Gómez, and J. Tejada, "Polynomial calculation of the Shapley value based on sampling," *Computers and Operations Research*, vol. 36, no. 5, pp. 1726-1730, 2009.

[27] J. Castro, D. Gómez, E. Molina, and J. Tejada, "Improving polynomial estimation of the Shapley value by stratified random sampling with optimum allocation," *Computers and Operations Research*, vol. 82, pp. 180-188, 2017.

[28] J. P. Christophersen, C. D. Ho, C. G. Motloch, D. Howell, and H. L. Hess, "Effects of reference performance testing during aging using commercial lithium-ion cells," *Journal of The Electrochemical Society*, vol. 153, no. 7, p. A1406, 2006.

[29] J. Kim, H. Chun, M. Kim, J. Yu, K. Kim, T. Kim, and S. Han, "Data-driven state of health estimation of Li-Ion batteries with RPT-reduced experimental data," *IEEE Access*, vol. 7, pp. 106987-106997, 2019.

[30] R. Weber, "Probabilistic values for games," Cowles Foundation Discussion Papers 471R, Cowles Foundation for Research in Economics, Yale University, 1977.

[31] S. Han, S. Han, and H. Aki, "A practical battery wear model for electric vehicle charging applications," *Applied Energy*, vol. 113, pp. 1100-1108, 2014.

[32] C. Zhou, K. Qian, M. Allan, and W. Zhou, "Modeling of the cost of EV battery wear due to V2G application in power systems," *IEEE Trans. on Energy Conversion*, vol. 26, pp. 1041-1050, July 2011.

Liyang Han received his B.S degree in energy engineering from Zhejiang University, China, in 2012, and his M.S. degree in civil engineering from Stanford University, CA, USA, in 2014. He recently finished his Ph.D. defense at the University of Oxford and is expecting to confirm his Ph.D. degree by October 2020. He joined the Energy Analytics and Markets (ELMA) group at the Technical University of Denmark (DTU) in July 2020 as a postdoctoral researcher. His research interests include prosumer-centric energy markets and data markets.

Thomas Morstyn received his B.Eng. (Hon.) degree from the University of Melbourne, Australia, in 2011, and his Ph.D. degree from the University of New South Wales, Australia, in 2016, both in electrical engineering. He is a Lecturer in Power Electronics and Smart Grids with the School of Engineering at the University of Edinburgh, and he is also a visiting fellow with the Oxford Martin School at the University of Oxford. His research interests include multi-agent control and market design for integrating distributed energy resources into power system operations.

Malcolm McCulloch received his B.Sc. (Eng.) and Ph.D. degrees in electrical engineering from the University of the Witwatersrand, Johannesburg, South Africa, in 1986 and 1990, respectively. In 1993, he joined the University of Oxford, Oxford, U.K., to head up the Energy and Power Group, where he is currently an Associate Professor with the Department of Engineering Science. He is active in the areas of electrical machines, transport, and smart grids. His work addresses transforming existing power networks, designing new power networks for the developing world, developing new technology for electric vehicles, and developing approaches to integrated mobility.